Interdiffusion of Linear and Branched Polyethylene in Microlayers Studied via Melting Behavior

T. Schuman,[†] E. V. Stepanov,[†] S. Nazarenko,[†] G. Capaccio,[‡] A. Hiltner,*[,†] and E. Baer[†]

Department of Macromolecular Science and Center for Applied Polymer Research, Case Western Reserve University, Cleveland, Ohio 44106, and BP Chemicals, Ltd., Applied Technology, Grangemouth, FK3 9XH, U.K.

Received December 2, 1997; Revised Manuscript Received April 14, 1998

ABSTRACT: Kinetics of interdiffusion of a miscible polymer pair, high density polyethylene (HDPE) and linear low density polyethylene (LLDPE), was studied experimentally in order to characterize the conditions required to construct gradient morphologies from microlayers. Microlayers were taken into the melt for a period of time, and the compositional gradient was fixed by crystallization upon quenching. High specific interfacial area of microlayers offset the low diffusion mobility of polymeric chains so that the microlayer system in the melt approached compositional homogeneity on a laboratory time scale. This specific pair of polymers with broad-molecular-weight distribution formed isomorphic blends upon crystallization from the melt. Thermal analysis of the quenched microlayered pair indicated systematic changes in the melting behavior with the composition gradient, which made it possible to quantify the progress of interdiffusion without chemical labeling. The thermograms were analyzed by applying a diffusion model formulated especially for a polydisperse system. The analysis revealed the role of different fractions and allowed us to extract the diffusion coefficients for elementary chains in the developing melt blend from the net kinetics of interdiffusion. It was confirmed that the molecular-weight dependence of the polyethylene chain diffusion coefficient follows reptation theory. The magnitudes of the diffusion coefficients and activation energy were found to correlate well with data of previous studies on monodisperse polyethylene species. An effect of the heterogeneous chain microstructure of LLDPE, in contrast to the homogeneous branch distribution of its monodisperse analogues, was revealed.

1. Introduction

Melt processes exist that make it possible to form two (or more) polymers into microlayered arrays with hundreds, sometimes thousands, of alternating layers where the individual layer thicknesses are on the order of microns or less.[1−3] The stringent flow conditions required for microlayer coextrusion provide a rare opportunity to combine miscible polymers on a small scale with little or no mixing. Microlayers of miscible pairs can be precursors to unique gradient structures. Heating into the melt state activates interdiffusion of polymer chains; the system gradually converts into a periodic gradient blend with compositional maxima and minima located in the centers of the initial layers.[4] Although the diffusion coefficients of macromolecules are extremely low, because the layer thickness is on the micron-size scale, the microscopic length of interdiffusion gives rise to significant changes in local composition on the time scale of minutes and hours. Resultant periodic concentration profiles are retained upon subsequent cooling. If one or both components crystallize, the composition gradient is overlayed with another gradient, one in the crystalline morphology, which in turn, can be varied by the crystallization conditions. Synergistic combination of these gradients creates many possibilities for developing unusual architectures.

One example demonstrates how gradient structures are produced by concurrent crystallization and interdiffusion of polycarbonate and a miscible, crystallizable copolyester.[5−7] The process exploits different rates of crystallization and interdiffusion when the system is taken above the glass-transition temperature. At temperatures where interdiffusion is much faster than crystallization, the composition gradually progresses toward homogeneity. However, if the time scales of interdiffusion and crystallization are comparable, the effect of the composition gradient on crystal nucleation and growth rates results in anisotropic spherulitic morphologies. The anisotropy can be controlled by coordinating conditions of time and temperature.

Because control of interdiffusion underlies the development of gradient structures, reliable prediction and modeling of the kinetics in real systems is of critical importance. Considerable progress has been made in understanding the mechanisms of macromolecular chain diffusion. Experiments performed on monodisperse species have provided information about chain diffusion coefficients for many materials.[8−10] This makes it possible to approach an understanding of the complex kinetics of mutual interdiffusion of polydisperse components under periodic boundary conditions inherent to microlayers. Because the chain diffusion coefficient is highly dependent on molecular weight, different fractions participate in the diffusional flux on different time scales. Consequently, partial spatial fractionation and dynamic redistribution of the molecular weight are anticipated.[11] Differences in the fractional diffusion coefficients of the components will result in convective flow and movement of the interface; this effect, similar to the Kirkendall effect in metals, has been demonstrated for polymers.[12,13] Furthermore, short and long chains play different roles in the processes of crystal nucleation and growth from the melt; these phenomena will affect the development of gradient crystalline morphologies.

* To whom correspondence should be addressed.
[†] Case Western Reserve University.
[‡] BP Chemicals, Ltd.

S0024-9297(97)01758-0 CCC: $15.00
Published on Web 06/24/1998

It is proposed that interdiffusion in microlayers of real polydisperse polymers can be monitored by a comparatively simple experimental method if the components cocrystallize. A single melting peak that shifts monotonically in temperature and a linear change of enthalpy with composition define the specific melting characteristics that tag the concentration of interdiffusing components of isomorphic blends. In this case, the melting thermogram contains a complete description of the spatial distribution of the components; this information can be extracted with appropriate models that describe the compositional profile on the scale of individual layers.

Examples of polymer pairs that are miscible in the melt and cocrystallize in an isomorphic structure are uncommon.[14] The similarity in chemical structure of polyethylene and its copolymers suggests that they would meet both these requirements. Estimates based on calculated equilibrium melting temperatures of high-density polyethylene (HDPE) and linear low-density polyethylene (LLDPE) blends indicate that the interaction parameter is almost zero.[15] This characteristic also eliminates any concentration dependence of the chain diffusion coefficient, so that the effect of polydispersity on interdiffusion will not overlap with, and be hidden by, accompanying factors. This combination of properties appears highly suitable for the proposed purpose.

Primary evidence for miscibility and cocrystallization of polyethylenes with the broad-molecular-weight distribution and branching heterogeneity typical of commercial resins comes from a single melting peak and a single set of X-ray reflections with no peak broadening.[16−19] Blends generally determined to cocrystallize are those of HDPE (density ca. 0.96) with LLDPE having at most 2 mol % branching (density ca. 0.92). This limit on the branch density of LLDPE for miscibility with HDPE is confirmed with model blends that employ fractions of HDPE blended with either fractions of LLDPE or narrow-molecular-weight hydrogenated or deuterated polybutadiene.[20−23]

In this study, polydisperse HDPE and LLDPE were combined as microlayers and subsequently formed into gradient structures by heating into the melt state. The progress of the composition gradient was followed by quenching from the melt and analyzing the melting thermogram of the cocrystallized components. Various analytical models were formulated and tested to obtain a satisfactory description of the gradient composition. The resulting diffusion coefficients were compared with published values for monodisperse linear and branched polyethylenes.

2. Materials and Methods

A high-density polyethylene resin (HDPE) and a linear low-density polyethylene resin (LLDPE) were provided by BP Chemicals, Ltd. The HDPE had the molecular weight of M_w = 316 600 g/mol and polydispersity = 15.7. The LLDPE comonomer was butene and the ethyl branch content was 20/1000 carbons. The LLDPE had the molecular weight of M_w = 118 000 g/mol and polydispersity = 4.2. The molecular-weight distributions, provided by the manufacturer, were well-approximated by a logarithmic normal distribution (Figure 1). The densities of compression-molded plaques were measured at room temperature using a gradient column (ASTM D 1505-85), the density of LLDPE was 0.922 g/cm^3 and the density of HDPE was 0.956 g/cm^3.

Microlayers of HDPE and LLDPE with 32 alternating layers were extruded in a 1:1 feed ratio using the microlayer coextrusion system described previously.[24,25] The extruder temperatures were chosen to match the viscosities of the two melt streams when they entered the coextrusion block. The melt temperature of HDPE was 320 °C and that of LLDPE was 140 °C. The flow rate from each extruder was 24 cm^3/min at 20 rpm. The layer-multiplying dies were at 200 °C. The contact time in the die assembly was estimated to be less than 15 s before the extrudate was quenched in water. The microlayer was extruded as a tape about 1-mm thick and 0.8-cm wide. The viscosity mismatch of HDPE and LLDPE in the die assembly, 6:1 at 200 °C, resulted in some layer nonuniformity. Because the lower viscosity LLDPE tended to encapsulate the edges, specimens for analysis were taken from the center of the tape.

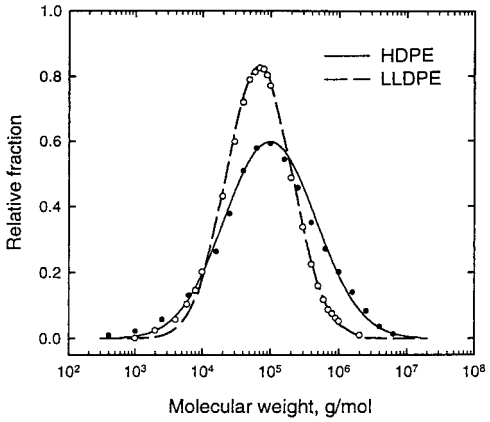

Figure 1. Molecular-weight distributions of LLDPE and HDPE shown as the experimental data (circles) and the Gaussian approximation (lines).

The HDPE and LLDPE were also dry-blended in various compositions and extruded in a Haake Rheodrive 5000 twin screw extruder at 200 °C and 20 rpm. The melt blends were subsequently extruded through the microlayer coextrusion system and used as controls.

A 6.6-mm circular disk was stamped from the center of the microlayer tape. Specimens this size fit snugly in the aluminum sample pans of the differential scanning calorimeter (DSC) and did not become distorted when melted. The pan lid was aligned with the extrusion direction to preserve sample orientation. Specimens were heated in the DSC at 200 °C/min to the desired temperature, held at that temperature for the desired time, and cooled at a rate of 40 °C/min. Zero minutes indicates that the specimen was taken to the melt temperature and cooled immediately.

The melt-treated specimen was removed from the DSC pan and halved normal to the extrusion direction. One of the halves was used for thermal analysis. Approximately one-third was trimmed from each side parallel to the extrusion direction. Specimens measuring about 2.2-mm × 0.8-mm × 1.0-mm thick and weighing about 2 mg were cut with a razor blade for differential scanning calorimetry analysis. The heating rate was 10 °C/min. The average composition from the enthalpy of melting was 58/42 w/w (HDPE/LLDPE) in the center third of the microlayer.

The other half of the melt-treated specimen was used for optical microscopy. Sections about 10-μm thick were microtomed from the entire cross-section with the cryogenic ultramicrotome. Phase contrast images were captured on video and the layer thicknesses were determined by image analysis. The layer thickness varied significantly as seen in the histograms in Figure 2. However, the profile of the layers in the microlayer tape cross-section did not change along the length of the tape. Variation in the thickness of individual layers and in the average layer thickness in this direction was less than 10%. Therefore, the composition and layer thicknesses were the same from one specimen to the next. The average layer thickness was 17.1 ± 7.4 μm for LLDPE and 24.8 ± 6.8 μm for HDPE. This yielded a composition of 59/41 w/w

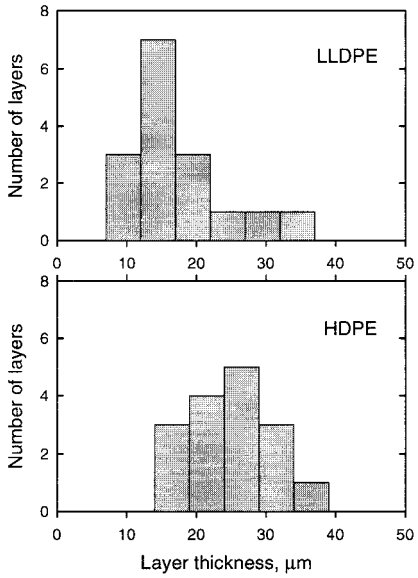

Figure 2. Statistical distribution of the layer thickness in microlayers.

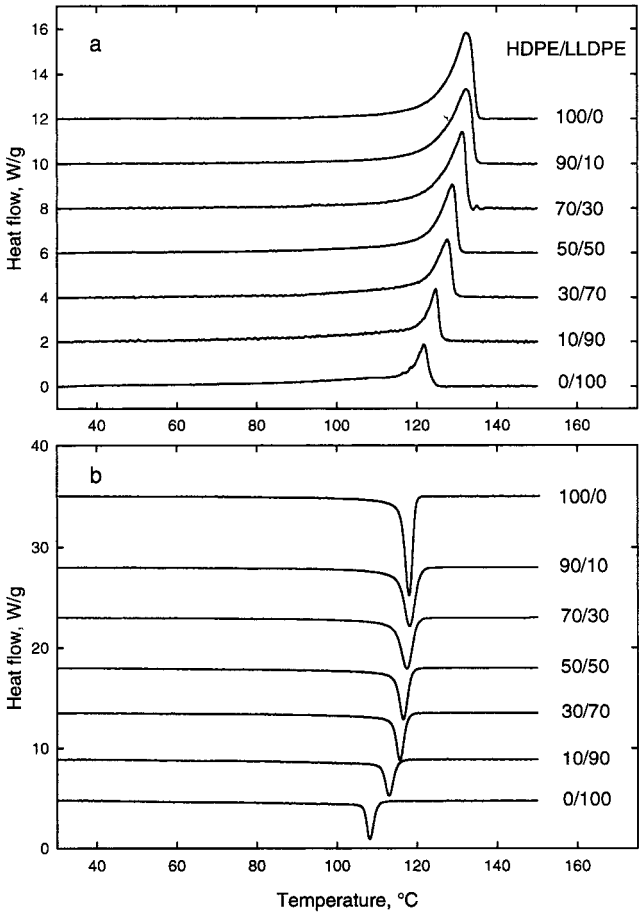

Figure 3. Melting (a) and crystallization (b) thermograms of HDPE/LLDPE melt blends of different compositions.

(HDPE/LLDPE). For analysis, the composition was taken as 60/40 (HDPE/LLDPE).

3. Results and Discussion

3.1. Crystallization of HDPE/LLDPE Blends. Figure 3 exhibits melting and crystallization thermograms of HDPE/LLDPE melt blends together with the thermograms of HDPE and LLDPE. Single melting and crystallization peaks were observed in the blends for all compositions irrespective of the cooling rate. A small shoulder on the low-temperature side of the LLDPE melting peak also appeared on the melting peak of the blends in proportion to the amount of LLDPE. The melting temperature and melting enthapy of the blends were intermediate between those of HDPE and LLDPE. The linear relationship between melting enthalpy and composition (Figure 4a) indicated additive contributions of HDPE and LLDPE to the total crystallinity. In contrast, the melting temperature showed pronounced nonlinear behavior (Figure 4b).

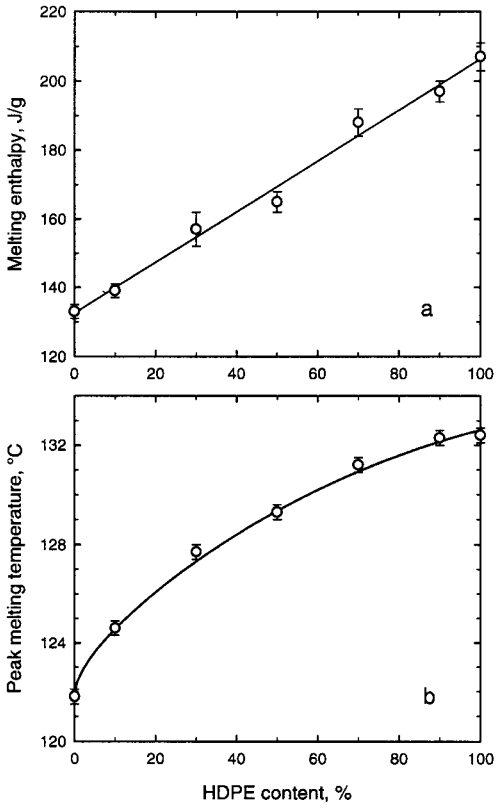

Figure 4. Dependence of the melting enthalpy (a) and the peak melting temperature (b) on the HDPE/LLDPE melt blend composition.

Single melting and crystallization peaks are an important feature of isomorphic blends. Gradual progression of the shape of the melting and crystallization peaks with composition is usually considered to be an indication of cocrystallization.[16−19] The two parameters that described the melting endotherm shape of the HDPE/LLDPE blends, the height and the half-width (defined as the width at half the peak height), varied linearly with composition. It therefore seemed possible to use the additivity features of enthalpy and peak shape to reconstruct the melting endotherm of any blend composition. To do this, the melting temperature of the blend was determined (Figure 4b); the endotherms of HDPE and LLDPE in Figure 5a were shifted to that temperature and added proportionally. The plots in Figure 5b−f compare the calculated thermogram, which is the sum of the proportional contributions of HDPE and LLDPE, with the measured endotherm. Because of the excellent agreement between calculated and experimental results, the reverse procedure could be used to deconvolute the melting endotherm of any blend into the contributions of HDPE and LLDPE in order to obtain the blend composition.

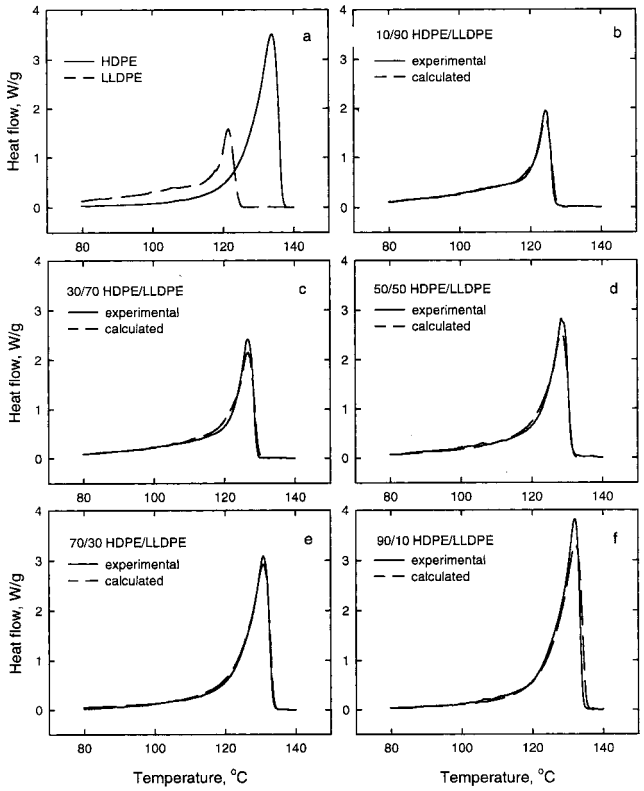

Figure 5. Comparison of the experimental blend melting thermograms to those calculated by linear superposition of HDPE and LLDPE control thermograms, both shifted to the blend melting temperature.

3.2. Interdiffusion in HDPE/LLDPE Microlayers. Optical micrographs of sections microtomed from the microlayer after it was annealed at 200 °C are shown in Figure 6. The layers were easily distinguished at this magnification even after a very long time in the melt. The reason that individual layers could still be observed after a melt history that should have made the system almost homogeneous was not immediately apparent. It later transpired that morphological features revealed the position of the interface,[26] but this became clear only after the role of the high-molecular-weight HDPE fraction was appreciated. Inspection of the cross-section indicated that the layer thicknesses remained unchanged if the melt time was less than about 100 min. After 600 min in the melt, the LLDPE layers were noticably thinner and the HDPE layers were noticably thicker. After a very long time in the melt, the LLDPE layers were so thin that the number of layers appeared to have been halved from 32 to 16.

The average layer thicknesses as a function of time in the melt are plotted in Figure 7. The error bars refer to the deviation among different specimens cut along the length of the microlayer tape. After about 100 min in the melt, perceptible movement of the boundaries in the direction of the faster diffusing component provided evidence of convective flow similar to the Kirkendall effect in metals. This occurs when highly mobile chains diffuse into the region of less mobile chains; the resulting osmotic pressure drives the bulk flow. The effect is most easily observed in polymers if the two components are monodisperse and widely differing in molecular weight.[12] Now, it is demonstrated that the effect can also be observed in polymers of normal molecular weight and molecular-weight distribution. The LLDPE and HDPE chosen for this study differed in average molecular weight and polydispersity sufficiently that domination of the diffusion kinetics by the more mobile LLDPE component was manifest at longer times.

The series of melting thermograms of the HDPE/LLDPE microlayer in Figure 8a,b show the effect of residence time in the melt at 150 and 200 °C. Initially, the microlayer exhibited two melting peaks with maxima at 123 and 131 °C, compared to those at 121.8 and 132.2 °C for LLDPE and HDPE with the same process and thermal history. This confirmed minimal mixing of the two polyethylenes during coextrusion. The gradual convergence of the two melting peaks toward a single peak as the time in the melt state increased reflected the progress of interdiffusion. A single peak was first observed after 270 min at 150 °C and after 105 min at 200 °C, consistent with a longer characteristic time of interdiffusion at 150 °C than at 200 °C. Additional time in the melt produced virtually no change in the melting temperature but served to sharpen the peak. The plot of peak half-width in Figure 9 shows that when the two melting peaks converged to a single peak, after approximately 100 min at 200 °C, the peak was still much broader than that of the corresponding melt blend. The peak continued to sharpen with time in the melt and approached the shape of the blend peak only after about 600 min. Clearly, the time required for the two melting peaks to converge into a single peak did not represent the interdiffusion endpoint of a homogeneous blend. Further analysis of the melting endotherm was required before the interdiffusion kinetics could be extracted from the thermal behavior.

3.3. Melting Endotherm of Partially Interdiffused Microlayers. The contact time between the layers in the layer multiplying dies was of the order of seconds prior to fast solidification of the melted structure. Thus, the opportunity for interdiffusion of HDPE and LLDPE during processing was brief. In the solid state the layered structure existed indefinitely without further change. Heating again to the melt state activated interdiffusion of the polymer chains; the extent of interdiffusion depended on the diffusion coefficient

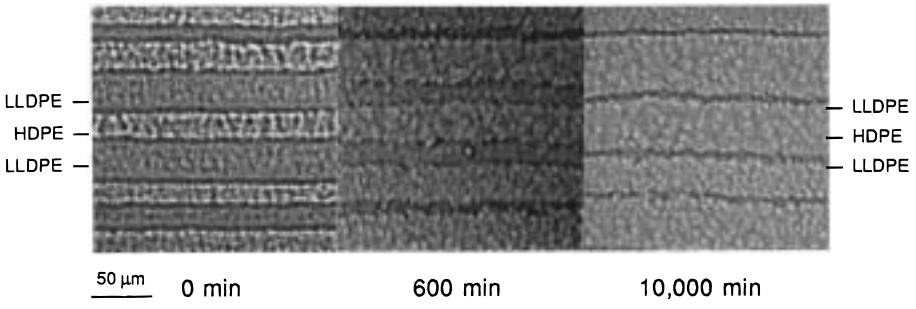

Figure 6. Optical micrographs of the layers after the microlayer were taken to 200 °C for the time indicated.

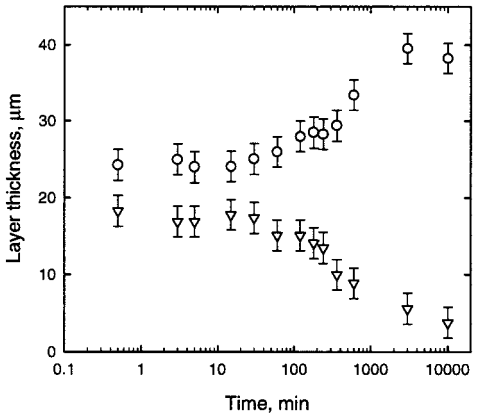

Figure 7. Change in the average HDPE (circles) and LLDPE (triangles) layer thickness with time at 200 °C.

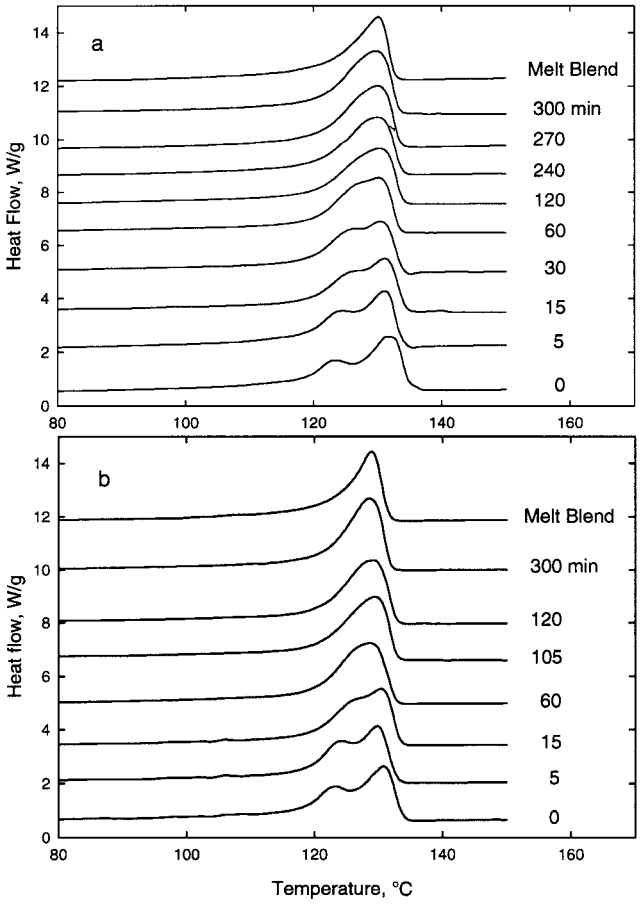

Figure 8. Examples of convergence of the microlayer thermograms to the melt blend single peak with increasing time at 150 °C (a) and 200 °C (b).

at the melt temperature and the time in the melt. Partial interdiffusion in a system of alternating layers resulted in periodic concentration profiles with minima and maxima located at the centers of layers. Crystallization of HDPE and LLDPE "froze" the composition profile during cooling and the subsequent heating thermogram revealed consecutive melting peaks of the LLDPE-rich and HDPE-rich layers. As the time in the melt state increased, the concentration profile gradually progressed toward a uniform composition equal to the overall system composition and a single sharp melting peak.

All the information about the composition profile is contained in the melting endotherm; however, it cannot

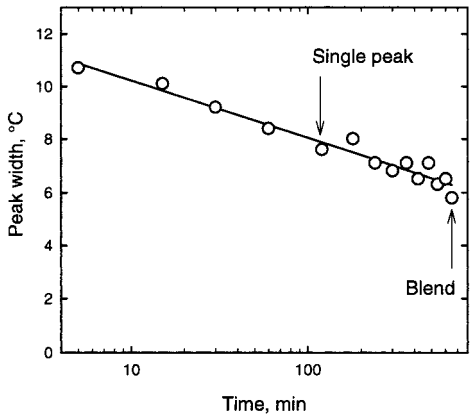

Figure 9. Decrease of the microlayer melting peak half-width with the time at 200 °C.

be extracted easily. A complete description of the melting transition of the partially interdiffused system would require a summation of the contributions of each infinitesimal element of the unknown periodic concentration profile. To make an analysis of the melting behavior possible, it is convenient to separate the composition profile into a series of interdiffusion elements, each consisting of one-half of an LLDPE layer together with one-half of the adjacent HDPE layer. Each interdiffusion element with a gradient composition is approximated by two homogeneous layers, both blends of LLDPE and HDPE, with compositions equal to the average compositions of the LLDPE and HDPE layers. Using additivity of the component contributions to the thermogram, the average compositions of the two blend layers can be obtained.

To deconvolute the experimental thermograms, a series of simulated thermograms of the LLDPE-rich layer with compositions from 0/100 to 60/40 (HDPE/LLDPE) at 0.02 intervals was developed by shifting the melting endotherms of LLDPE and HDPE to the melting temperature of the blend (Figure 4b) and superposing them as exemplified in Figure 5. The thermogram of the complementary HDPE-rich layer was constructed similarly, and superposition of the pair of thermograms was weighted according to the 60/40 (HDPE/LLDPE) composition. Several examples in Figure 10 show simulated melting endotherms of partially interdiffused microlayers.

The difference between the peak melting temperatures, ΔT_m, was used to characterize the progress of interdiffusion. The experimental endotherms were matched with the simulated ones to find the closest correspondence. However, if two maxima were clearly distinguishable in the thermogram, ΔT_m was generally measured directly. If the peaks were strongly overlapping so that only one maximum appeared in the thermogram, the endotherms were matched with the simulated ones, generally using the half-width to determine the best fit. Areas of all simulated and experimental endotherms were confirmed to be the same as required by linearity between enthalpy and composition.

3.4. Description with a Simple Diffusion Model. The experimental dependence of ΔT_m on the melt residence time at 200 °C is shown in Figure 11. Different symbols represent three separate series of measurements. Data were also generated for melt temperatures of 150, 175, and 225 °C. The initial analysis followed the simplest approach, that interdiffusion was characterized by a single mutual diffusion

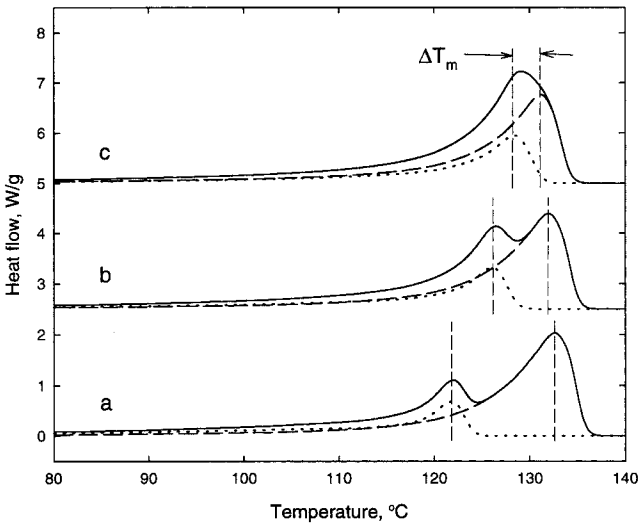

Figure 10. Examples of deconvolution of the microlayer melting thermogram by superposition of the HDPE-rich and LLDPE-rich layer thermograms as described in the text. The HDPE/LLDPE composition in the LLDPE-rich layer is 0/100 (a), 20/80 (b), and 40/60 (c); the composition of the HDPE-rich layer is complementary in accordance with 60/40 overall composition.

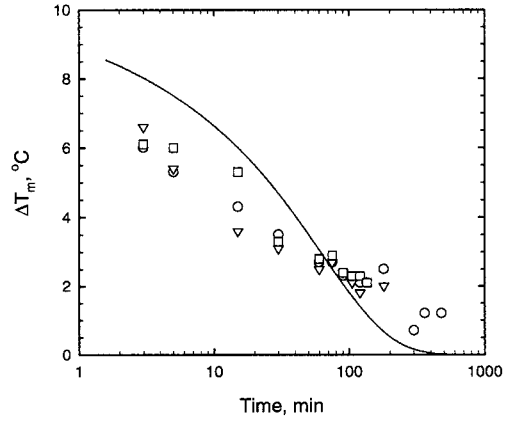

Figure 11. Dependence of the microlayer melting peak separation on the time at 200 °C (symbols) and the best fit by the simple interdiffusion model (line). The symbol shapes represent different experimental series.

coefficient D that depended on temperature only. Such a model successfully described the change in glass-transition temperature as microlayers of polycarbonate and a miscible copolyester were annealed above the glass-transition temperature.[5,7]

The interdiffusion element of total thickness L_0 was defined as one-half of an LLDPE layer L_1 together with one-half of the adjacent HDPE layer L_2, so that $L_0 = L_1 + L_2$. The dimensionless position of the interface was $l = L_1/L_0$, considering the center of an LLDPE layer as the origin. In this approach, average bulk thicknesses of the layers were used; hence, l was determined by the overall LLDPE/HDPE composition in the microlayer. The concentration profile was described by a one-dimensional diffusion equation:

$$\frac{\partial W_i}{\partial t} = D\frac{\partial^2 W_i}{\partial x^2} \qquad (1)$$

where $i = 1, 2$ for LLDPE and HDPE respectively, W_i is the weight concentration of the component i, t is the time, and x is the coordinate. Accounting for the initial condition of a sharp interface with complete separation of the components, and zero composition gradient at both boundaries of the interdiffusion element, the solution of eq 1 took the form

$$W_1(x,t) = \frac{L_1}{L_0} + \sum_{n=1}\frac{2}{n\pi}\sin\left(n\pi\frac{L_1}{L_0}\right)\cos\left(n\pi\frac{x}{L_0}\right)\exp\left(-\frac{n^2\pi^2 D}{{L_0}^2}t\right) \qquad (2)$$

and $W_2(x,t)$ is complementary to unity. The average LLDPE content in the LLDPE-rich layer was obtained by integrating eq 2 from 0 to L_1. The average composition of the HDPE-rich layer followed directly from the overall composition in the interdiffusion element. From the average composition, the melting temperature of each layer was obtained using the experimental dependence (Figure 4b), and the diffusion coefficient was considered as a fitting parameter for the dependence $\Delta T_m(t)$.

An example of the best fit by the least-squares method is shown in Figure 11 (solid line). The model did not fit the experimental results very well at 200 °C, nor did the model fit any better for other melt temperatures. At short times, the fast drop of the measured ΔT_m indicated that diffusion occurred more rapidly than predicted by the simple model, and the opposite deviation at long times implied a comparatively slow diffusion rate. This behavior was generally consistent with diffusion of components with a broad-molecular-weight distribution because shorter chains diffused more rapidly than the average and long chains more slowly. Involvement of different fractions in the interdiffusion process on different time scales smoothed the dependence $\Delta T_m(t)$. The molecular-weight distributions of HDPE and LLDPE were much wider than those of the polymer pair used previously to develop the simple diffusion model (polycarbonate and the miscible copolyester with $M_n/M_w \approx 2$ for both).[5] A more refined model was required to account for the effect of polydispersity in HDPE/LLDPE microlayers.

3.5. Diffusion Model for a Polydisperse System. The molecular-weight distributions of LLDPE and HDPE, $G_1(M)$ and $G_2(M)$, are displayed in logarithmic coordinates in Figure 1. As seen, polydispersity was rather high; the fractions spread out over more than 2 orders in magnitude of molecular weight from about 10^4 to higher than 10^6. The diffusion coefficient of a polymer chain strongly depends on molecular weight; hence, the time scale of interdiffusion for the fractions can differ in several orders of magnitude. Such a considerable difference obviously affected the net kinetics of interdiffusion observed by the melting temperature shift.

To account for polydispersity, diffusion of each molecular-weight fraction was considered separately. Because both components were polyethylenes, their melt densities and the densities of their blends in the melt were assumed to be the same and independent of molecular weight. Additionally, the interaction parameter χ could be taken as zero for this system.[15] There is some discussion in the literature concerning possible small but finite values of χ.[27−29] Finite interaction would add a concentration (ϕ)-dependent term of about

$\chi N\phi$ relative to the undisturbed chain diffusion coefficient,[12] where $N \cong 100$ is the number of monomer units and $0 < \phi < 1$. Even if $\chi \cong 5 \times 10^{-4}$, as proposed recently for lightly branched polyethylenes,[29] the correction would be no more than 1−2%. Thus, diffusion of each fraction could be considered as proceeding independently from other fractions of the same component as well as from all fractions of the other component. This is also consistent with previous observations that the diffusion coefficient of a monodisperse species in a polyethylene matrix is not affected by the matrix molecular weight if the latter is 2−3 times higher than the critical entanglement molecular weight.[8,30]

Accordingly, the fractional diffusion coefficient was determined by molecular weight only. For this dependence, the ordinary power law was used:[8−10]

$$D_{M,i} = D_{0,i}\left(\frac{\overline{M}_i}{M}\right)^{\alpha} \tag{3}$$

where $D_{M,i}$ is the diffusion coefficient for the fraction of component i with molecular weight M, $\overline{M}_i$ is the component i weight-average molecular weight, and $D_{0,i}$ is the diffusion coefficient of chains of the average molecular weight chosen as a reference. The power α characterizes the sharpness of the molecular-weight dependence of the diffusion coefficient and takes values from 1 to 3 for various systems.[8,10] Values around $\alpha = 2$, which follows from reptation theory,[31,32] are commonly reported for diffusion of polyethylenes.[30,33−39]

The net diffusional flux of each component toward the other is determined by summation of the fractional fluxes. Because of different molecular-weight distributions and diffusion coefficients, the net fluxes, in general, will not match each other. Convective flow of the melt compensates for the mass loss and ensures the density conservation. Experimentally, convective flow reveals itself by movement of the interface toward the faster diffusing component.[12,13] For the system under investigation, the shrinkage of LLDPE layers at longer times (Figures 6 and 7) was an indication of the moving interface. However, as seen by comparison of Figure 7 with Figure 11, the shift of the interface was significant only at times longer than 300 min at 200 °C, when the value of $\Delta T_m \leq 1$ °C indicated that the components were almost completely intermixed. Thus, the interface could be assumed to be stationary during the characteristic interdiffusion time of the major fractions of both components. The mismatch of the diffusional fluxes appeared only at the longer time scale corresponding to diffusion of high-molecular-weight fractions, which represented a small percentage of the total amount of material. Because the high-molecular-weight tail was significantly larger in the HDPE distribution than in the LLDPE distribution, immobility of long HDPE chains at times when the LLDPE concentration had flattened was compensated by convective mass flow of the HDPE layer.

The observed stability of the interface during the characteristic time of ΔT_m convergence justified the use of an equation similar to (1) for the fractional fluxes:

$$\frac{\partial w_{M,i}}{\partial t} = D_{M,i}\frac{\partial^2 w_{M,i}}{\partial x^2} \tag{4}$$

where $i = 1, 2$ for LLDPE and HDPE respectively and $w_{M,i}$ is the weight concentration of the fraction of component i with molecular weight M divided by its initial value $\rho G_i(M)$ (the density ρ is assumed to be the same for both components). Equation 3 was solved on the interval of the interdiffusion element $0 < x < L_0$ with initial and boundary conditions that assumed total separation of the components on the interface at L_1 at zero time, and no flux out of the interdiffusion element:

$$w_{M,i}(x,t=0) = (-1)^i\theta(x - L_1)$$
$$\left.\frac{\partial w_{M,i}}{\partial x}\right|_{x=0,L_0} = 0 \tag{5}$$

where $\theta(x)$ is the Heaviside's step function. Incorporating the molecular weight dependence given by eq 3, the solution of eq 4 took the following following form:

$$w_{M,1}(x,t) = h\left(\frac{L_1}{L_0},\frac{x}{L_0},\frac{t}{\tau_{M,1}}\right)$$
$$w_{M,2}(x,t) = h\left(1 - \frac{L_1}{L_0},1 - \frac{x}{L_0},\frac{t}{\tau_{M,2}}\right) \tag{6}$$

where the function

$$h(l,x',t') = l + \sum_{n=1}\frac{2}{n\pi}\sin(n\pi l)\cos(n\pi x')\exp[-n^2 t'] \tag{7}$$

describes the shape of the fractional concentration profile in terms of the dimensionless coordinate x' and time t';

$$\tau_{M,i} = \frac{{L_0}^2}{\pi^2 D_{0,i}}\left(\frac{M}{\overline{M}i}\right)^{\alpha} \tag{8}$$

represents the characteristic time for diffusion of the fraction. Total concentration profiles are defined by integration over the fractions:

$$W_i(x,t) = \int_M w_{M,i}(x,t)\, G_i(M)\, \mathrm{d}M \tag{9}$$

and the net diffusional fluxes of the components through the interface are determined by the following relationship:

$$J_i(t) = -\rho\int_M D_{M,i}\left[\frac{\partial w_{M,i}}{\partial x}\right]_{x=L_1} G_i(M)\, \mathrm{d}M \tag{10}$$

The solution, given in eqs 6−9, is not rigorously consistent with local density conservation $W_1 + W_2 \equiv 1$ if the components are of different polydispersities $G_i(M)$. The same is true even for a weaker condition $J_1 + J_2 = 0$ which describes conservation in density averaged over each layer. Some convective flow must always occur in a polydisperse system. Neglect of this flow is possible only at the specific ratio of the diffusion coefficients $D_{0,i}$ that yields the best match of the component diffusional fluxes. Persistence of a stationary interface, as observed visually, determines the time scale over which this assumption is valid for this system. Violation of the local density conservation is also minimized in this way.

To formulate a condition which could replace the exact local density conservation requirement, we minimized

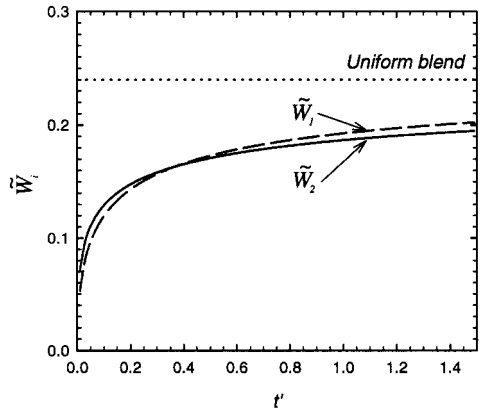

Figure 12. Normalized amount of HDPE (solid line) and LLDPE (dashed line) that crossed the interface in time t' referred to the characteristic interdiffusion time for the weight-average fraction. The dotted line shows the asymptotic value for both functions corresponding to complete intermixing.

deviation of the interface from its initial position over a characteristic time scale of interdiffusion. Because of the total flux continuity, the interface velocity $\dot{l}$ is defined by the following equation:

$$\rho\dot{l} = J_1 + J_2 \tag{11}$$

and the interface shift is determined by the difference $\Delta\overline{W}$ between the following quantities:

$$\overline{W}_i(t) = (-1)^{i+1}\frac{1}{\rho}\int_0^t J_i(t')\,\mathrm{d}t' \tag{12}$$

which represent the amount of component i that has crossed the interface from each side in time t. If ΔW is relatively small, eqs 6−10 can be used to calculate $\overline{W}_i(t)$. In these terms, the condition is formulated as the requirements that the quantity

$$\int_0^\tau (\overline{W}_1(t) - \overline{W}_2(t))^2\,\mathrm{d}t \tag{13}$$

take a minimum during a characteristic time τ if varying the diffusion coefficients, and $\Delta\overline{W}/\overline{W}_i \ll 1$ when calculated at the minimum. Expression 13 can be reduced to functions of dimensionless variables by referring the diffusion coefficients and the characteristic time to those of one of the components: $s = D_{0,2}/D_{0,1}$ and $t' = t/\tau_{0,1}$, where $\tau_{0,1} = L_0^2/\pi^2 D_{0,1}$, and defining $H_1(t') = \overline{W}_1(t'\tau_{0,1})$ and $H_2(st') = \overline{W}_2(t'\tau_{0,1})$. Performing the minimization over s, the condition is formulated as a parametric integral equation:

$$\int_0^1 (H_1(t') - H_2(st'))(t'J_2(st') - H_2(st'))\,\mathrm{d}t' = 0 \tag{14}$$

The solution of the equation gives the ratio of the diffusion coefficients s which is most consistent with a stationary interface in a polydisperse system.

Equation 14 was solved numerically with the molecular-weight distributions $G_i(M)$ shown in Figure 1 and the exponent $\alpha = 2$. The value $s = 0.48$ was obtained for the ratio between the LLDPE and HDPE weight-average fraction diffusion coefficients. Using this value, the dynamics of interdiffusion is shown in Figure 12 in terms of normalized functions $\tilde{W}_i(t') = \overline{W}_i(t'\tau_{0,1})/L_0$. In accordance with eq 11, the difference $\Delta\tilde{W}$ between these functions shows the interface shift relative to the total

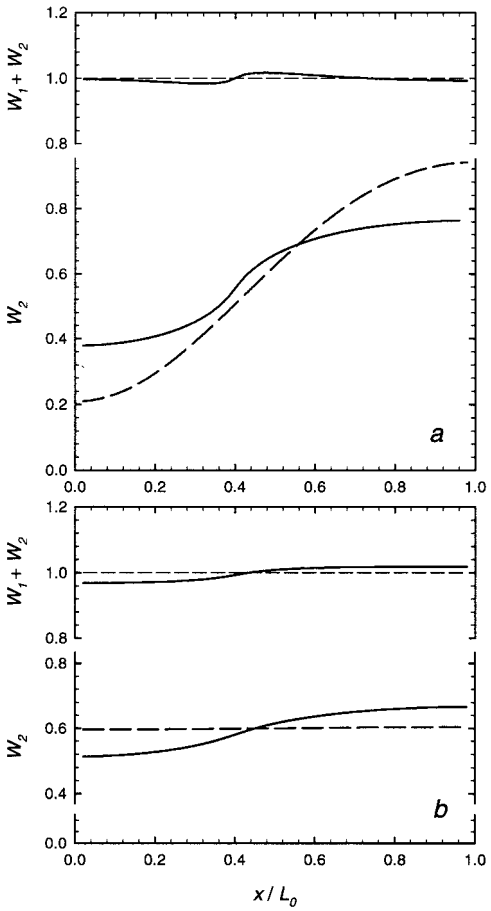

Figure 13. The HDPE concentration profile over an interdiffusion element, W_1, and the sum of both component concentrations, $W_1 + W_2$, as calculated by the polydisperse (solid line) and the simple (dashed line) models at short (a) and long (b) times.

length of the interdiffusion element. As seen, the curves almost coincide, and the difference between them varies within a value of 0.02 (0.5 μm in real length), which is much less than the experimental accuracy (Figure 7). At times $t' \gg 1$, the curves increasingly diverge so that the amount of HDPE diffused into the LLDPE layer is less than that of LLDPE diffused into the HDPE layer. This causes the interfaces on either side of an LLDPE layer to move toward each other. Thus, the LLDPE layer appears to shrink, in accordance with the experimental observations.

Calculation of the component concentration profiles $W_i(x,t)$ with the resultant value of the ratio $D_{0,2}/D_{0,1}$ tested how consistent solutions (6)−(9) were with local density conservation. At $t' < 1$, the identity $W_1 + W_2 \equiv 1$ was fulfilled within a 1−2% accuracy. Figure 13a shows the concentration profile of HDPE, W_2, and the total concentration $W_1 + W_2$ calculated at $t' = 0.5$. To illustrate the effect of polydispersity, the profile is compared with that calculated with the simple model at the same time, assuming the diffusion coefficient D in the simple model is equal to the diffusion coefficient of the weight-average fraction $D_{0,1}$. Comparison for long interdiffusion times ($t' = 5$) is made in Figure 13b. At short times, rapid diffusion of the low-molecular-weight chains is responsible for the more shallow profile in the polydisperse model compared to that in the simple model. Conversely, the concentration gradient persists at long times in the polydisperse model because diffusion of the high-molecular-weight chains is very slow.

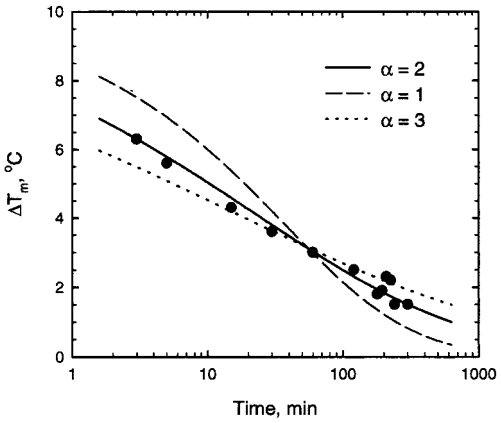

Figure 14. Dependence of the microlayer melting peak separation on the time at 175 °C (symbols) and the best fit by the polydisperse model with various exponents α in the molecular-weight dependence of the diffusion coefficient.

The total concentration profile $W_1 + W_2$ at long times shows a regular trend to rarefaction of the LLDPE layer and densification of the HDPE one, which gives rise to the compensating convective flow toward the LLDPE layer as discussed above.

3.6. Description with the Polydisperse Diffusion Model. An application of the model to the description of the experimental data was made by calculating the average compositions of the LLDPE and HDPE layers. In terms of the HDPE content, they were $\overline{W_2}/L_1$ and $1 - \overline{W_2}/(L_0 - L_1)$, respectively. The LLDPE content was considered as complimentary to unity at the ratio of the diffusion coefficients $s = 0.48$ obtained above. Because the stability of the interface during a characteristic time of melting temperature convergence was observed at all temperatures in the range 150−225 °C, the difference in the temperature dependencies of the diffusion coefficients $D_{0,i}$ was assumed to be insignificant, and this value of s was used for all temperatures. The melting temperatures corresponding to the average compositions were determined and the melting peak separation ΔT_m was compared with experimental results. The diffusion coefficient $D_{0,1}$ was considered as a fitting parameter.

At first, the fit of the model to the experimental data was examined with different integer values of the power α in the molecular-weight dependence of the diffusion coefficient, eq 3. The best fit is exemplified in Figure 14 for α = 1, 2, 3 using data of one experimental series for diffusion at 175 °C. Excellent agreement was found only for α = 2. Other values gave rise to larger deviations between the model and the experiment. This result was in full agreement with previous measurements of the diffusion coefficient performed on monodisperse polyethylene species of different molecular weights.[30,33−39]

The data were fit for a quadratic molecular-weight dependence of the fractional diffusion coefficient, eq 3, in eqs 6−9. The model calculations were made with the actual distribution of layer thicknesses (Figure 2), so that the bulk kinetics was defined by summation over 16 interdiffusion elements with the parameters L_0 and L_1 measured for each layer. An average value of $D_{0,1}$ was obtained at each temperature by independently fitting three separate series of measurements. Comparison of the experimental data with a theoretical curve corresponding to the average value of $D_{0,1}$ for each

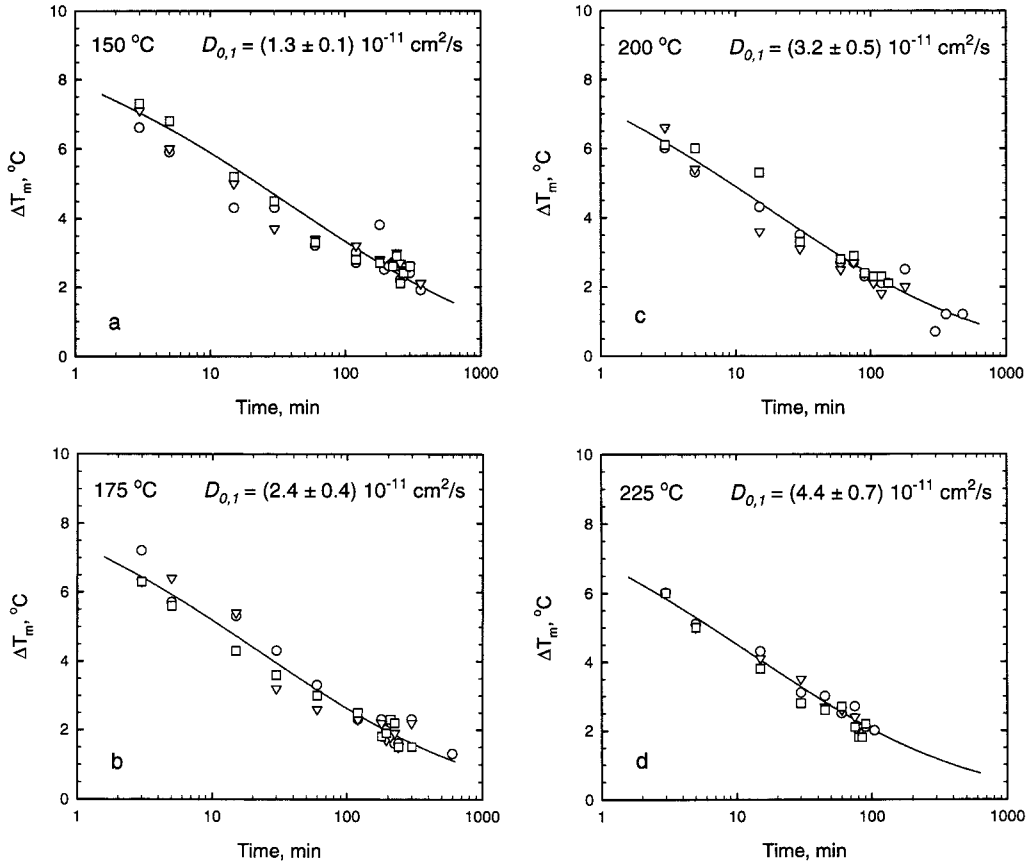

Figure 15. Dependencies of the microlayer melting peak separation on the time at different temperatures (symbols) and the fits by the polydisperse model with the diffusion coefficients indicated on the plots (lines). The symbol shapes represent different experimental series.

Table 1. Diffusion Coefficients for Polyethylene Chains

materials (diffusant/matrix)	method	M_w, kg/mol (diffusant)	M_w/M_n (diffusant)	T, °C	D^* (reported)[c]	E_a, kJ/mol	D^* (175 °C)[c]	refs
			18−20 ethyl branches per 1000 °C					
dPB/hPB[a]	SANS[d]	48−214	1.02−1.03	125	0.23 ± 0.02	26	0.58	33, 40
				145	0.33 ± 0.02			
				165	0.50 ± 0.02			
dPE/HDPE[b]	IRMD[e]	3.6−23	1.8−2.25	176	0.34 ± 0.05		0.34	36, 37
dPB/HDPE[b]	IRMD[e]	2.6−96	1.02−1.06	176	0.82 ± 0.11		0.82	34, 35
dPB/hPB	SIRM[f]	1.25−303.6	1.03−1.05	170	0.54 ± 0.01		0.58	30
dPB/hPB	FRES[g]	424	1.05	125	0.20		0.52	41
hPB	NMR[h]	1−75	1.02−1.07	175	0.59 ± 0.03		0.59	43
LLDPE	NMR[h]	10.9	1.2	200	1.1 ± 0.1		0.74	42
		30.3	1.18					
LLDPE/(HDPE + LLDPE)	MMTC[i]	118	4.2	150	0.18 ± 0.01	28	0.33	present study
				175	0.33 ± 0.05			
				200	0.45 ± 0.07			
				225	0.61 ± 0.09			
			Linear					
HDPE	NMR[h]	0.59−4.1	1.08−1.14	175	1.65 ± 0.05		1.65	38
		13.6−119.6	1.11−1.19					
HDPE	NMR[h]	0.3−20	1.1−1.5	150	2.3 ± 0.1	28[j]	3.7	39
				200	5.7 ± 0.2	26, 21[k]		
HDPE	NMR[h]	4.42−70.1	1.11−1.36	200	1.5 ± 0.6		1.0	42
HDPE/(HDPE + LLDPE)	MMTC[i]	316.6	15.7	150	0.62 ± 0.05	28	1.1	present study
				175	1.1 ± 0.2			
				200	1.6 ± 0.2			
				225	2.1 ± 0.3			

[a] Multilayered from solution. [b] HDPE matrix: $M_w = 160$ kg/mol, $M_w/M_n = 16$. [c] cm^2 mol^2/s g^2. [d] Small-angle neutron scattering. [e] Infrared microdensitometry. [f] Scanning infrared microscopy [g] Forward recoil spectroscopy. [h] Pulsed field gradient NMR technique. [i] Microlayer melting temperature convergence. [j] Series of different M_w species at two temperatures. [k] Temperature scan of one M_w species.

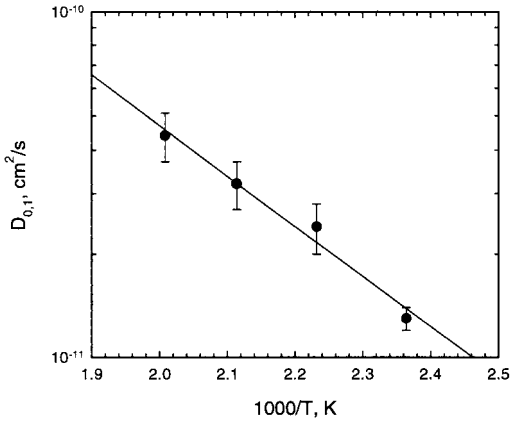

Figure 16. Temperature dependence of the diffusion coefficient for the average molecular-weight LLDPE fraction.

temperature is shown in Figures 15a−d. The relatively small deviation in $D_{0,1}$ was consistent with good reproducibility of the experimental data. The diffusion coefficients are presented in Figure 16 in the form of an Arrhenius plot. The slope of the linear regression line on the plot determines an activation energy, which was found to be $E_a = 28 \pm 3$ kJ/mol.

Several aspects of the analysis deserve further discussion. If the number of layers is large, it becomes cumbersome to use individual L_0 values for the model calculations, and it would be convenient to substitute an average value even in instances where significant nonuniformity of layer thickness exists. As seen by inspection of eqs 6−9, layer thickness L_0 is included into the time dependence of the local concentration profile as the product with molecular weight $\tau_{M,i} \propto (L_0 M)^2$, which then is averaged over fractions with function (7) in eq 9. Because the variation in L_0 is no more than a factor of 2 whereas the molecular weight varies by 2 orders of magnitude, the shape of the $\Delta T_m(t)$ curve is determined by the polydispersity. To evaluate the effect of thickness variation, the fit of the experimental data was performed by eqs 6−9, but assuming the interdiffusion elements to be of equal length L and the interface position l to be defined by the average composition and considering the ratio $D_{0,1}/L^2$ as a fitting parameter. Theoretical curves calculated in this way were almost indistinguishable from those presented in Figure 15. In this approach, L and $D_{0,1}$ are not obtained independently, but as the product $D_{0,1}/L^2$. Substituting $1/L^2$ by the average $\langle(1/L_0)^2\rangle$ as determined from the actual statistical distribution of the layer thicknesses L_0 (Figure 2) gave practically the same result for $D_{0,1}$ as the individual L_0 values, whereas the average $\langle L_0\rangle$ resulted in a $D_{0,1}$ about 20% smaller.

Comparison of the diffusion coefficients with literature data for polyethylenes is presented in Table 1. Many of the measurements were performed with hydrogenated polybutadiene (hPB) labeled by either partial deuteration (dPB) or carbon isotope (for NMR studies). The material was prepared by anionic polymerization with subsequent solution hydrogenation in order to obtain species highly monodisperse in molecular weight. Those studies where the molecular weight was systematically varied over the range indicated in Table 1 consistently determined the value of the exponent in the molecular-weight dependence of the diffusion coefficient as $\alpha = 2$. Using this exponent, it is convenient to compare results for different molecular weights in terms of the so-called prefactor D^*, defined as the ratio D/M^2, where D is the diffusion coefficient for chains of molecular weight M.[8,10] The values of the prefactor calculated on the basis of the reported data are pre-

sented in Table 1. Finally, the prefactors were reduced to the same reference temperature 175 °C by assuming an activation energy of 28 kJ/mol.

The chemical structure of chains produced by hydrogenation of polybutadiene is usually assumed to resemble that of a linear branched polyethylene with 18−20 ethyl branches per thousand carbon atoms which are distributed uniformly along the chain.[44,45] The LLDPE used in the present study had the same average concentration of ethyl branches; therefore, it seemed appropriate to compare the prefactor calculated from the diffusion coefficient $D_{0,1}$ with that measured for hPB. As seen in Table 1, the prefactor obtained in this work is of the same order of magnitude; however, the value is lower than that for hPB, even taking into account the scatter among the literature data. This difference can be readily understood by considering that LLDPE is a real material with nonuniform distribution of branches along a chain and differences between the branch content of low- and high-molecular-weight chains. The occasional concentration of branches in one portion of the chain can act as an anchor to increase local friction and hamper reptation.

Results of NMR studies on diffusion of linear polyethylene chains in monodisperse fractions of HDPE correlate well with the present study. The NMR data show significant variation among the different experiments which can be ascribed to the high sensitivity of the method to polydispersity of the species.[38] Nevertheless, the prefactor obtained for HDPE is systematically higher than that for LLDPE and hydrogenated polybutadienes, which reveals the role of branches in the reptation mechanism of diffusion.

In summary, we exploited the microlayer technique to study interdiffusion of real polydisperse polyethylenes without using a chemical label. Previously, this innovative approach had only been demonstrated qualitatively[4] and quantitatively for a polymer pair with polydispersity low enough that a single diffusion coefficient sufficed in the analysis.[5−7] In the present study, we used a specific pair of miscible polyethylenes, one linear and one lightly branched. Melting thermograms of their blends of all compositions revealed additive contributions of the components. In this case, the indirect technique of DSC was effective for monitoring the complex kinetics of interdiffusion. We showed that polydispersity does not always mean a moving boundary, even though the diffusion coefficient depends strongly on molecular weight. In retrospect, this is not surprising; however, the result considerably facilitated analysis of the interdiffusion process and extraction of the characteristic parameters. Our findings indicate that the time scale for homogenization of miscible systems depends more on the molecular-weight distribution, especially the high-molecular-weight tail, and less on the size scale of the phases. This result has implications to the kinetics of heat sealing of polymer films. The study also demonstrates the feasibility of creating gradient morphologies from microlayers on an accessible time scale.

Acknowledgment. This research was generously supported by BP Chemicals, Ltd., the Army Research Office (Grant DAAL03-92-G-0241), and the National Science Foundation (Grant DMR97-05696).

References and Notes

(1) Im, J.; Baer, E.; Hiltner, A. *High Performance Polymers*; Baer, E., Moet, A., Eds.; Hanser: Munich, 1991; pp 175−198.
(2) Sung, K.; Hiltner, A.; Baer, E. *J. Mater. Sci.* **1994**, *29*, 5559.
(3) Pan, S. J.; Im, J.; Hill, M. J.; Keller, A.; Hiltner, A.; Baer, E. *J. Polym. Sci., Part B: Polym. Phys.* **1990**, *28*, 1105.
(4) Keskkula, H.; Paul, D. R. *J. Appl. Polym. Sci.* **1987**, *34*, 1861.
(5) Pollock, G.; Nazarenko, S.; Hiltner, A.; Baer, E. *J. Appl. Polym. Sci.* **1994**, *52*, 163.
(6) Haderski, D.; Nazarenko, S.; Hilner, A.; Baer, E. *Macromol. Chem. Phys.* **1995**, *196*, 2545.
(7) Nazarenko, S.; Haderski, D.; Hiltner, A.; Baer, E. *Macromol. Chem. Phys.* **1995**, *196*, 2563.
(8) Kausch, H. H.; Tirrell, M. *Annu. Rev. Mater. Sci.* **1989**, *19*, 341.
(9) Tirrell, M. *Rubber Chem. Technol.* **1984**, *57*, 523.
(10) Green, P. F. *Diffusion in Polymers*; Neogi, P., Ed.; Marcel Dekker: New York, 1996; pp 251−302.
(11) Keith, H. D.; Padden, F. J., Jr. *J. Polym. Sci., Part B: Polym. Phys.* **1987**, *25*, 229.
(12) Kramer, E. J.; Green, P.; Palmstrom, J. *Polymer* **1984**, *25*, 473.
(13) Wu, S.; Chuang, H.-K.; Han, C. D. *J. Polym. Sci., Part B: Polym. Phys.* **1986**, *24*, 143.
(14) Utracki, L. A. *Polymer Alloys and Blends*; Hanser: Munich, 1989; pp 57−63.
(15) Pracella, M.; Benedetti, E.; Galleschi, F. *Thermochim. Acta* **1990**, *162*, 163.
(16) Hu, S.-R.; Kyu, T.; Stein, S. *J. Polym. Sci., Part B: Polym. Phys.* **1987**, *25*, 71.
(17) Hay, J. N.; Zhou, X.-Q. *Polymer* **1993**, *34*, 2282.
(18) Datta, N. K.; Birley, A. W. *Plast., Rubber Compos. Process Appl.* **1982**, *2*, 237.
(19) Edwards, G. H. *Br. Polym. J.* **1986**, *18*, 88.
(20) Alamo, R. G.; Glaser, R. H.; Mandelkern, L. *J. Polym. Sci., Part B: Polym. Phys.* **1988**, *26*, 2169.
(21) Graessley, W. W.; Krishnamoorti, R.; Balsara, N. P.; Butera, R. J.; Fetters, L. J.; Lohse, D. J.; Schulz, D. N.; Sissano, J. A. *Macromolecules* **1994**, *27*, 3896.
(22) Defoor, F.; Groeninckx, G.; Reynaers, H.; Schouterden, P.; van der Heijden, B. *J. Appl. Polym. Sci.* **1993**, *47*, 1839.
(23) Rhee, J.; Crist, B. *Macromolecules* **1991**, *24*, 5663.
(24) Mueller, C. D.; Nazarenko, S.; Ebeling, T.; Schuman, T. L.; Hiltner, A.; Baer, E. *Polym. Eng. Sci.* **1997**, *37*, 355.
(25) Mueller, C. D.; Kerns, J.; Ebeling, T.; Nazarenko, S.; Hiltner, A.; Baer, E. *Polymer Process Engineering 97*; Coates, P. D., Ed.; The Institute of Materials: London, 1997; pp 137−157.
(26) Schuman, T.; Stepanov, E. V.; Nazarenko, S.; Hiltner, A.; Baer, E., to be published.
(27) Alamo, R. G.; Londono, J. D.; Mandelkern, L.; Stehling, F. C.; Wignall, G. D. *Macromolecules* **1994**, *27*, 411.
(28) Schipp, C.; Hill, M. J.; Barham, P. L.; Cloke, V. M.; Higgins, J. S.; Oiarzabal, L. *Polymer* **1996**, *37*, 2291.
(29) Crist, B.; Hill, M. J. *J. Polym. Sci., Part B: Polym. Phys.* **1997**, *35*, 2329.
(30) von Seggern, J.; Klotz, S.; Cantow, H.-J. *Macromolecules* **1991**, *24*, 3300.
(31) de Gennes, P.-G. *Scaling Concepts in Polymer Physics*; Cornell University Press: Ithaca, NY, 1979.
(32) Doi, M.; Edwards, S. F. *The Theory of Polymer Dynamics*; Oxford University Press: Oxford, 1986.
(33) Bartels, C. R.; Crist, B.; Graessley, W. W. *Macromolecules* **1984**, *17*, 2702.
(34) Klein, J.; Fletcher, D.; Fetters, L. J. *Faraday Symp. Chem. Soc.* **1983**, *18*, 159.
(35) Klein, J.; Fletcher, D.; Fetters, L. J. *Nature* **1983**, *304*, 526.
(36) Klein, J.; Briscoe, B. J. *Proc. R. Soc. London A* **1979**, *365*, 53.
(37) Klein, J. *Philos. Mag. A* **1981**, *43*, 771.
(38) Pearson, D. S.; Ver Strate, G.; von Meerwall, E.; Schilling, F. C. *Macromolecules* **1987**, *20*, 1133.
(39) Bachus, R.; Kimmich, R. *Polymer* **1983**, *24*, 964.
(40) Bartels, C. R.; Graessley, W. W.; Crist, B. *J. Polym. Sci.: Polym. Lett.* **1983**, *21*, 495.
(41) Crist, B.; Green, P. F.; Jones, R. A. L.; Kramer, E. J. *Macromolecules* **1989**, *22*, 2857.
(42) Fleischer, G. *Colloid Polym. Sci.* **1987**, *265*, 89.
(43) Pearson, D. S.; Fetters, L. J.; Graessley, W. W.; Ver Strate, G.; von Meerwall, E. *Macromolecules* **1994**, *27*, 711.
(44) Rachapidy, H.; Smith, G. G.; Raju, V. R.; Graessley, W. W. *J. Polym. Sci., Part B: Polym. Phys.* **1979**, *17*, 1211.
(45) Tanzer, J. D.; Bartels, C. R.; Crist, B.; Graessley, W. W. *Macromolecules* **1984**, *17*, 2708.
MA971758E